Quantification of early nonpharmaceutical interventions aimed at slowing transmission of Coronavirus Disease 2019 in the Navajo Nation and surrounding states (Arizona, Colorado, New Mexico, and Utah)

Short Title: The COVID-19 epidemics in the Navajo Nation and surrounding states

Ely F. Miller[1], Jacob Neumann[1#], Ye Chen[2], Abhishek Mallela[3†], Yen Ting Lin[4], William S. Hlavacek[5], Richard G. Posner[1*]

[1]Department of Biological Sciences, Northern Arizona University, Flagstaff, Arizona, United States of America

[2]Department of Mathematics and Statistics, Northern Arizona University, Flagstaff, Arizona, United States of America

[3]Department of Mathematics, University of California, Davis, California, United States of America

[4]Computer, Computational, and Statistical Sciences Division and Center for Nonlinear Studies, Los Alamos National Laboratory, Los Alamos, New Mexico, United States of America

[5]Theoretical Division and Center for Nonlinear Studies, Los Alamos National Laboratory, Los Alamos, New Mexico, United States of America

[†]Current address: Theoretical Division and Center for Nonlinear Studies, Los Alamos National Laboratory, Los Alamos, New Mexico, United States of America

[#]Current address: Department of Chemistry and Chemical Biology, Cornell University, Ithaca, New York, United States of America

[*]Corresponding author. Email: richard.posner@nau.edu

Abstract: During an early period of the Coronavirus Disease 2019 (COVID-19) pandemic, the Navajo Nation, much like New York City, experienced a relatively high rate of disease transmission. Yet, between January and October 2020, it experienced only a single period of growth in new COVID-19 cases, which ended when cases peaked in May 2020. The daily number of new cases slowly decayed in the summer of 2020 until late September 2020. In contrast, the surrounding states of Arizona, Colorado, New Mexico, and Utah all experienced at least two periods of growth in the same time frame, with second surges beginning in late May to early June. To investigate the causes of this difference, we used a compartmental model accounting for distinct periods of non-pharmaceutical interventions (NPIs) (e.g., behaviors that limit disease transmission) to analyze the epidemic in each of the five regions. We used Bayesian inference to estimate region-specific model parameters from regional surveillance data (daily reports of new COVID-19 cases) and to quantify uncertainty in parameter estimates and model predictions. Our results suggest that NPIs in the Navajo Nation were sustained over the period of interest, whereas in the surrounding states, NPIs were relaxed, which allowed for subsequent surges in cases. Our region-specific model parameterizations allow us to quantify the impacts of NPIs on disease incidence in the regions of interest.

Keywords: Severe Acute Respiratory Syndrome Coronavirus 2 (SARS-CoV-2), Ordinary Differential Equations (ODEs), Mathematical Model, Statistical Inference, Markov Chain Monte Carlo (MCMC).

Introduction

An outbreak of pneumonia of unknown cause starting in Wuhan, China was recognized in late December 2019 and widely reported in early January 2020 [1, 2]. The disease was later named Coronavirus Disease 2019 (COVID-19) [1]. The causative agent was identified as a novel coronavirus, later named Severe Acute Respiratory Syndrome Coronavirus 2 (SARS-CoV-2). COVID-19 rapidly spread to other countries [1, 2, 3], and the World Health Organization (WHO) declared the COVID-19 outbreak a pandemic on March 11, 2020 [4]. In the United States (US), during the early months of the pandemic, two regions were severely affected as measured by cumulative number of COVID-19 cases per capita: *Diné Bikéyah*, more commonly known as the Navajo Nation, and New York City.

On May 18, 2020, the Navajo Nation had the highest cumulative number of COVID-19 cases per hundred thousand in the US (2,344 cases per 100,000 residents), surpassing the New York City metropolitan statistical area (MSA), which had 1,806 cases per 100,000 residents [5,6]. Remarkably, both regions significantly slowed the transmission of COVID-19 and prevented additional surges in new COVID-19 cases until late September 2020 while many other regions, including the states of Arizona, Colorado, New Mexico, and Utah, each experienced a series of two surges in cases during the same period [6].

The President of the Navajo Nation and the Governors of the surrounding states of Arizona, Colorado, New Mexico, and Utah independently issued guidance and mandates to control the spread of COVID-19. These non-pharmaceutical interventions (NPIs) enforced or encouraged an array of behaviors that putatively protect susceptible individuals from SARS-CoV-2 infection, such as curtailing of travel, reduction in face-to-face interaction, face mask-wearing, working from home, etc. Although the governmental actions across the five regions

were similar, there were notable differences, particularly in the duration of mandates, as we will discuss later. The disease transmission dynamics in the five regions were also different. In the Navajo Nation, the number of new cases detected daily rose sharply in late March to early April, peaked in May, and then steadily declined until late September 2020 [7]. In contrast, in each of the surrounding states, there were at least two periods of growth in new cases between 01-March-2020 and 14-September-2020 [6].

Insights into why the Navajo Nation experienced only a single period of growth in new COVID-19 cases during the period of interest while neighboring regions experienced two distinct phases of increasing case counts could point to strategies for controlling transmission of diseases similar to COVID-19 in the future. A possible explanation for the difference between the Navajo Nation (with one phase of growth in disease incidence) and the surrounding states (each with two phases of growth in disease incidence) is that NPIs were more effective and/or more sustained in the Navajo Nation. To evaluate this hypothesis, for each of the five regions of interest, we sought to use region-specific daily case reporting data to infer parameters of a compartmental model for COVID-19 transmission that accounts for subpopulations of susceptible individuals protected or not from SARS-CoV-2 infection by NPIs. The model structure allows for multiple phases, or periods, of NPIs. Each phase is associated with three parameters: an onset time, a sum of rate constants that defines a timescale for transition to a setpoint level of adoption of disease-avoiding behaviors, and the setpoint (the fraction of the regional population adopting disease-avoiding behaviors). We have previously shown that this model is able to reproduce the dynamics of regional COVID-19 epidemics in 2020 in 280 of 384 MSAs in the US [8], including the 15 most populous metropolitan areas [7], and in all 50 states [9].

We adopted a Bayesian inference approach enabled by Markov chain Monte Carlo (MCMC) sampling to obtain samples of region-specific parameter posteriors. Inferences were conditioned on one to three periods of NPIs, uniform proper priors, a negative binomial model for surveillance noise, estimates of selected parameters taken to have the same values across all regions of interest [7], and were based on daily counts of new cases available from January 21 to September 14, 2020. Following Lin et al. [7], we used model selection to determine the most parsimonious number of NPI periods. A model structure and parameterization were thus found for each region of interest. Each parameterization allows the model with selected structure to explain the corresponding regional epidemic curve. The parameter posteriors found indicate that NPIs were not more effective but were more sustained in the Navajo Nation than in the surrounding states.

Methods

The COVID-19 surveillance data used to parameterize the model for the Navajo Nation was obtained from the *Navajo Times* COVID-19 webpage [5]. The *Navajo Times* provided daily reports of new confirmed COVID-19 cases over the period of interest. The reported source of this information was the Navajo Nation Department of Health (NNDOH) [10]. The COVID-19 surveillance data used to parameterize the models for Arizona, Colorado, New Mexico, and Utah were obtained from a GitHub repository maintained by *The New York Times* newspaper [11]. This GitHub repository collects new case reports from local health agencies in the United States. For each of the four states, we aggregated county-level case counts to obtain state-level case counts.

Information and data used to compare NPI mandates in each of the four states neighboring the Navajo Nation were obtained from the *John Hopkins Coronavirus Resource*

Center [12]. This NPI resource webpage collects state-wide NPI mandates issued by each US state's governor and plots when they were issued against daily new cases to visualize the effect of NPIs on trends in new COVID-19 cases. The *John Hopkins Coronavirus Resource Center* collects policy data from various state-specific websites such as state and governor websites and from the National Governors Association. It should be noted that information in this resource characterizes state-level mandates only; information about county-level mandates is less readily available and was not considered in this study. Information about NPI mandates in the Navajo Nation was obtained from the NNDOH public website [10]. Using policy data collected by *John Hopkins Coronavirus Resource Center* and reported by the NNDOH, we compared governmental mandates in the Navajo Nation and the four surrounding states.

The model we considered in this study is that of Lin et al. [7]. It is a compartmental model that divides a regional population of interest into susceptible (S), exposed (E), infectious (I), and removed (R) compartments (Fig 1). Exposed persons transition through a series of five stages, introduced to capture the distribution of incubation times observed for COVID-19 [13]. The model also accounts for quarantine, self-isolation because of symptom awareness, hospitalization, and death. Importantly, persons are allowed to transition between two modes of behavior, in which they are either protected (imperfectly) from infection (because of adoption of disease-avoiding behaviors) or are mixing freely (i.e., taking no special precautions to prevent infection). The model tracks 25 compartments and each compartment corresponds to an ordinary differential equation (ODE). There is an auxiliary 1-parameter measurement model, which relates the variables of the compartmental model to reported new cases through surveillance testing [7]. The equations of the mechanistic compartmental model and the measurement model can be found in Appendix 1 of Lin et al. [7].

The model accounts for an initial phase of NPIs beginning at time $t = \sigma$, where σ is fixed to the date the region of interest accumulated at least 200 COVID-19 cases. The model can be extended to account for n additional periods. Thus, the total number of NPI periods considered in a regional model is given by $n + 1$ [7]. The start of a new NPI phase is accompanied by step changes in the values of the three NPI parameters. In the models for the Navajo Nation (NN), Arizona (AZ), Colorado (CO), New Mexico (NM), and Utah (UT), we considered three possible settings for n (the number of additional NPI periods beyond the initial period): $n = 0$ (only one NPI period over the entire period of interest), $n = 1$ (two NPI periods), and $n = 2$ (three NPI periods). The setting for n was determined as described below.

To determine the structure of the compartmental model for each region of interest (i.e., the number of distinct NPI phases), we used a heuristic model-selection method. In this approach, we calculated the value of the Akaike information criterion corrected for small sample size ($AICc$) for n and $n + 1$ versions of the model, where $n = 0, 1$. We also calculated the value of the Bayesian information criterion (BIC) for the same two versions of each model. ΔAICc is defined as the change in $AICc$ between n and $n + 1$ versions of the models: $\Delta AICc = AICc^{n} - AICc^{n+1}$. ΔBIC is defined similarly: $\Delta BIC = BIC^{n} - BIC^{n+1}$. We adopted $n + 1$ over n when both of the following conditions held true: $\Delta AICc > 10$ and $\Delta BIC > 10$. The method of model selection described above was used to decide between the use of $n = 0$ and $n = 1$, and between the use of $n = 1$ and $n = 2$ [7, 14].

In the case of only an initial NPI period ($n = 0$), the compartmental model and auxiliary measurement model have 20 parameters combined. Five of the parameters are considered adjustable; these parameters are all region-dependent. The other 15 parameters are taken to have

fixed values. The 15 fixed parameters are S_0, σ, I_0, m_b, ρ_E, ρ_A, k_L, k_Q, j_Q, f_A, f_H, f_R, c_A, c_I, and c_H. The parameter S_0 represents the total population of the region of interest, as determined by census data [15], which we took to be fixed. I_0 refers to the starting number of infected individuals. We used $I_0 = 1$. ρ_E and ρ_A refer to the relative infectiousness of exposed persons and asymptomatic persons, respectively, compared to symptomatic persons [16, 17]. Infected persons are taken to enter quarantine with rate constant k_Q and persons with symptoms and mild disease are taken to self-isolate with rate constant j_Q. Persons in the protected subpopulation (i.e., persons adopting disease-avoiding behaviors) are taken to be less likely to acquire or transmit disease by a factor m_b. In the model, the incubation period is divided into 5 stages. Movement from one stage to the next occurs with rate constant k_L [13]. The fraction of exposed persons who never become symptomatic is represented by f_A. The fraction of symptomatic persons who progress to severe disease (and hospitalization or isolation at home) is represented by f_H [18]. The fraction of persons with severe disease who recover is represented by f_R. Persons with asymptomatic disease leave the immune clearance stage of infection and recover with rate constant c_A [19]. Persons with mild symptomatic disease recover with rate constant c_I [20]. Persons with severe disease recover with rate constant c_H [21]. The five adjustable parameters are t_0, p_0, λ_0, β, and f_D. The parameter t_0 refers to the start time of local sustained COVID-19 transmission; p_0 is the initial non-zero value of $P_\tau(t)$, the stationary fraction of the local population that is practicing disease-avoiding behaviors; λ_0 is the initial non-zero value of $\Lambda_\tau(t)$, a sum of rate constants that establishes a time scale for the establishment of the quasi-stationary state of NPIs; β is the disease transmission rate constant (or contact rate parameter) in the absence of NPIs; and f_D is the fraction of new infections detected in surveillance. The parameter f_D characterizes the effectiveness of surveillance and relates new cases to new infections. In the

model, $P_\tau(t)$ and $\Lambda_\tau(t)$ are taken to be step functions. Each of these functions has a value of 0 until $t = \sigma$ and thereafter changes value at a set of n times (if $n > 0$), denoted $\tau = \{\tau_1 > \sigma, \ldots, \tau_n > \tau_{n-1}\}$. The value of n starts at 0 and is incremented through model selection as described above. There is one additional adjustable parameter, r, the dispersion parameter of a negative binomial distribution $NB(p, r)$ used to characterize noise in case detection [7]. The value of r is inferred jointly with the five adjustable model parameters.

In the case of one additional NPI period beyond the initial period ($n = 1$), three more adjustable parameters are used, which are denoted τ_1, p_1, and λ_1. The latter two parameters determine the new values of $P_\tau(t)$, and $\Lambda_\tau(t)$ at time $t = \tau_1$, the start time of the second phase of NPIs. In general, three more adjustable parameters are added to the model each time n is incremented. The equations of the compartmental model and of the auxiliary model can be found in Appendix 1 of Lin et al. [7].

Bayesian inference of adjustable region-specific model parameter values was based on new daily case count data for NN, AZ, CO, NM, or UT. MCMC sampling was performed to obtain samples of the parameter posterior. We used an adaptive MCMC sampling algorithm described earlier [22] and implemented in the PyBioNetFit software package [23]. PyBioNetFit job setup files for the inferences performed in this study, including data files, are available online (https://github.com/lanl/PyBNF/tree/master/examples/Miller2022NavajoNation). We quantified uncertainty in daily case reports through resampling of the parameter posteriors so as to generate a posterior predictive distribution for daily number of new cases detected [7].

Results

The objective of our study was to quantify the effect of early non-pharmaceutical interventions (NPIs) on the transmission of COVID-19 in the Navajo Nation (NN) and surrounding states: Arizona (AZ), Colorado (CO), New Mexico (NM), and Utah (UT). We achieved this by applying Bayesian inference enabled by Markov chain Monte Carlo (MCMC) sampling to obtain posterior samples for NPI parameters of a mechanistic region-specific compartmental mathematical model for each region of interest (Figure 1). Inference was based on COVID-19 daily confirmed case count data. Because we set out to quantify the effectiveness of early NPIs during the emergence of SARS-CoV-2 in the US, we used case data available for the period starting on 21-January-2020 and ending on 14-September-2020.

The model we used to analyze data from the NN and surrounding states is illustrated in Figure 1. The model accounts for movement between different states of protection against SARS-CoV-2 infection because of disease-avoiding behaviors. In the model, persons are allowed to be in three states of protection: a state in which an uninfected person is protected imperfectly against infection because of disease-avoiding behaviors, a state in which an uninfected person is more exposed to infection because they do not take any special precautions to avoid infection, and a state in which an infected person is quarantined or in self-isolation. In the model, an initial NPI period ($n = 0$) begins as soon as the number of cumulative cases reaches or exceeds 200. A new NPI period is introduced through the model-selection procedure described in Methods. When a new NPI period is introduced, n is incremented and NPI parameters change.

Figure 2 and Figure 3 show 95% credible intervals of posterior predictive distributions for daily case detection for the NN and the four surrounding states. Posterior predictive distributions were found by drawing from parameter posterior samples generated through MCMC sampling, thereby propagating parametric uncertainty into prediction uncertainty. In the

posterior predictive distributions, NN only has surge in disease incidence whereas the surrounding states each have at least two surges.

Figure 2 and Figure 3 show curves for the daily number of new symptomatic infections (vs. cases) based on maximum a posteriori (MAP) estimates for parameters (which are equivalent to maximum likelihood estimates because of the use of uniform proper priors). In our calculations, the number of detected cases over a 1-d period is taken to be a fraction f_D of the number of new symptomatic infections generated during that same period. The value of f_D is region-specific. The MAP estimate for f_D is 0.2 for the Navajo Nation, 0.15 for Arizona, 0.35 for Colorado, 0.04 for New Mexico, and 0.07 for Utah.

Figure 2 and Figure 3 indicate when distinct NPI periods were determined to have begun. Table 1 summarizes results of the model-selection procedure used to decide between 1 or 2 or more NPI phases for each region of interest. The Navajo Nation was the only region of interest to have $\Delta AICc$ and ΔBIC values indicating only one NPI phase.

Figure 4 shows the marginal posteriors of the setpoint parameters $\{p_0, \ldots, p_n\}$ for each region, which were generated by MCMC sampling. Recall that each of these parameters determines the quasi-stationary population fraction adopting disease-avoiding behaviors and that there is a distinct setpoint for each distinct NPI phase (e.g., p_0, p_1, and p_2 for a region with three distinct NPI phases). For the Navajo Nation, we inferred only a single NPI phase over the period of interest. This phase is characterized by a NN-specific value for the setpoint parameter p_0. The marginal posterior for p_0 for the NN is shown in Figure 4A. In surrounding states, we inferred changes in adherence to disease-avoiding behaviors, i.e., different setpoints over time. The marginal posteriors for the state-specific setpoint parameters are shown in Figures 4B–4E.

Comparison of the marginal posteriors for different NPI phases within a given state reveals a significant relaxation in disease-avoiding behaviors in each state. Figure 5 shows MAP estimates for NPI setpoint parameters (e.g., p_0) for each region of interest over time. A higher setpoint indicates a higher prevalence of disease-avoiding behaviors. For the period of interest, we found that all regions experienced a decrease in their setpoint parameter values after an initial NPI phase except the Navajo Nation. Although Arizona, Colorado, and Utah initially had a higher setpoint than the Navajo Nation, the Navajo Nation maintained the initial setpoint for a longer period in comparison to the surrounding states.

Figure 6 shows Navajo Nation COVID-19 case data from 21-January-2020 to 5-February-2021 and projections of daily case counts for selected NPI scenarios after 14-September-2020. Between 21-January-2020 and 14-September-2020, the Navajo Nation maintained disease-avoiding behaviors (as characterized by the setpoint parameter p_0) and experienced only one surge in COVID-19 cases. However, after this period, the Navajo Nation experienced an additional surge in COVID-19 cases. The solid red curve in Figure 6 is the trajectory corresponding to the MAP estimate of p_1, obtained using data collected after 14-September-2020, and the dotted curves are different hypothetical trajectories based on lower and higher values for the NPI parameter p_1. We found that the Navajo Nation would have needed to maintain a value for p_1 greater than 0.27 after 14-September-2020 to avoid a surge in disease transmission.

Figure 7 presents a timeline of governmental mandates between 21-January-2020 and 14-September-2020 in the Navajo Nation and the four surrounding states. Four mandates are considered, which are related to face mask wearing, mass gatherings, non-essential business closures, and weekend lockdowns. As can be seen, these mandates were in effect for the longest

duration in the Navajo Nation. Mandates in surrounding states were in effect for shorter durations and were imposed less consistently.

Discussion

In this study, we used a compartmental model to quantify the overall effect of non-pharmaceutical interventions (NPIs) on COVID-19 transmission in specific regions, namely the Navajo Nation and the four surrounding states. The model for a given region includes a set of NPI setpoint parameters, each of which represents the quasi-stationary fraction of the regional population that is practicing disease-avoiding behaviors for a given period. By using surveillance data (daily case counts) to infer the region-specific values of the NPI setpoint parameters, we quantified the relative overall effectiveness of NPIs across the regions of interest. We detected changes in disease-avoiding behaviors over time using a model selection procedure, which indicates when an NPI setpoint needs to change value for consistency with surveillance data. A limitation of our approach is that we cannot ascertain the relative effectiveness of individual NPIs. Another limitation is that our model can only explain surges in disease incidence by relaxation of NPIs. The model does not account for other factors that could cause surges, such as increased disease transmissibility associated with emergence of a viral variant or loss of immunity.

From 21-January-2020 to 14-September-2020, we found that the Navajo Nation maintained the initial NPI setpoint throughout this period (Figure 4 and Figure 5), consistent with a single surge in COVID-19 incidence (Figure 2). In contrast, we found that the surrounding states of Arizona, Colorado, New Mexico, and Utah did not. That is, each surrounding state had two or more NPI phases, marked by different NPI setpoints and multiple surges in COVID-19 incidence. These findings are consistent with a comparison of governmental mandates across the

five regions of interest (Figure 7). Sustained NPIs is unique to the Navajo Nation and suggests an explanation for why this region experienced only one surge in COVID-19 cases while other regions experienced multiple surges.

Interestingly, we inferred that the fraction of the NN population adopting disease-avoiding behaviors upon initial implementation of NPIs was lower than that in Arizona, Colorado, and Utah and similar to that in New Mexico. These results implicate sustained NPIs (rather than effectiveness of NPIs) as the reason for the different disease transmission dynamics between the Navajo Nation (only a single surge in disease incidence) and the surrounding states (multiple surges).

Our results suggest that NPIs, even if only partially adopted, can slow and control disease transmission if mandates are consistent and are not relaxed prematurely or to too great an extent. We determined that the Navajo Nation's NPI setpoint parameter value between 21-January-2020 and 14-September-2020 was 0.35 but the value changed to 0.19 after 14-September-2020, in concert with a second surge in disease incidence. We determined the minimum NPI setpoint parameter value needed to maintain control of disease transmission (i.e., to avoid a surge in disease incidence) to be 0.27 (Figure 6). In other words, the second surge could have been prevented if 27% of the population had maintained disease-avoiding behaviors after 14-September-2020.

We inferred two other notable differences between the regions of interest beyond differences in adoption of effective NPIs. First, surveillance efforts may have had different levels of effectiveness. Our MAP estimates for f_D, the fraction of new infections detected, ranged from a low of 0.04 for New Mexico to a high of 0.35 for Colorado. Colorado, New Mexico, and Utah had similar numbers of cases per 100,000 residents but the inferred differences in surveillance

effectiveness suggest that COVID-19 impacts were significantly greater in New Mexico and Utah than in Colorado. Second, there were differences in contagiousness across the regions of interest. Our MAP estimates for β, the contact rate parameter, ranged from just over 0.3 per day for the Navajo Nation and New Mexico to just over 0.5 per day for Arizona. Using the formula for the basic reproduction number R_0 given by Mallela et al. [9], these differences in β estimates translate into the following estimated R_0 values for the five regions: 3.6 for New Mexico, 3.7 for the Navajo Nation, 4.4 for Utah, 4.6 for Colorado, and 5.9 for Arizona. Thus, the relatively high adoption of effective NPIs in Arizona was offset by relatively high transmission of COVID-19. Our analysis does not provide insight into why contagiousness varied across the regions of interest.

In summary, our analysis suggests that once NPIs have brought an outbreak under control, relaxation of the NPIs can be implemented but relaxation should be gradual to avoid a new surge in disease incidence. A relatively low level of disease incidence is not an indicator that NPIs can be safely relaxed. Moreover, a model accounting for NPIs can perhaps be used to guide relaxation of NPIs in a controlled manner.

Acknowledgments

YC, WSH, EFM, JN, and RGP acknowledge support from the National Institute of General Medical Sciences of the National Institutes of Health (grant R01GM111510). AM acknowledges support from the 2020 National Science Foundation Mathematical Sciences Graduate Internship Program and the Center for Nonlinear Studies at Los Alamos National Laboratory. WSH and YTL acknowledge support from the Laboratory Directed Research and Development Program at Los Alamos National Laboratory (project 20220268ER). We acknowledge use of the Monsoon computer cluster at Northern Arizona University, which is funded by Arizona's Technology and Research Initiative Fund.

Author Contributions

Conceptualization: EFM, WSH, RGP

Data Curation: EFM

Formal Analysis: EFM

Funding Acquisition: WSH, RGP, YC, AM, YTL

Investigation: EFM

Methodology: EFM, JN, AM, WSH, YTL

Project Administration: WSH, RGP

Resources: RGP

Software: EFM, JN, YTL

Supervision: RGP, WSH, YC

Validation: EFM, AM

Visualization: EFM

Writing – Original Draft Preparation: EFM, WSH, RGP

Writing – Review & Editing: EFM, JN, YC, AM, YTL, WSH, RGP

References

1. Gorbalenya AE, Baker SC, Baric RS, de Groot RJ, Drosten C, Gulyaeva AA, et al. The species severe acute respiratory syndrome-related coronavirus: classifying 2019-nCoV and naming it SARS-CoV-2. Nat Microbiol. 2020.
2. Holshue ML, DeBolt C, Lindquist S, Lofy KH, Wiesman J, Bruce H, et al. First case of 2019 novel coronavirus in the United States. New England Journal of Medicine. 2020;382(10):929–36.
3. The Covid Tracking Project [Internet]. Available from: https://covidtracking.com/
4. Cucinotta D, Vanelli M; CDV. Who declares COVID-19 a pandemic [Internet]. Acta bio-medica: Atenei Parmensis. U.S. National Library of Medicine. Available from: https://pubmed.ncbi.nlm.nih.gov/32191675/
5. COVID-19 Across the Navajo Nation [internet]. Available from: https://navajotimes.com/coronavirus-updates/covid-19-across-the-navajo-nation/
6. Coronavirus in the U.S.: Latest map and case count - The New York Times [Internet]. Available from: https://www.nytimes.com/interactive/2021/us/covid-cases.html
7. Lin YT, Neumann J, Miller EF, Posner RG, Mallela A, Safta C, et al. Daily forecasting of regional epidemics of coronavirus disease with Bayesian uncertainty quantification, United States. Emerging Infectious Diseases. 2021;27(3):767–78.
8. Mallela A, Lin YT, Hlavacek WS. Differential contagiousness of respiratory disease across the United States [Internet]. medRxiv. Cold Spring Harbor Laboratory Press; 2022. Available from: https://www.medrxiv.org/content/10.1101/2022.09.15.22279948v1

9. Mallela A, Neumann J, Miller EF, Chen Y, Posner RG, Lin YT, et al. Bayesian inference of state-level COVID-19 basic reproduction numbers across the United States. Viruses. 2022;14(1):157.
10. Dikos Ntsaaígíí-19 (COVID-19) [Internet]. Navajo Nation Department of Health. Available from: https://www.ndoh.navajo-nsn.gov/COVID-19
11. New York Times. COVID-19-data: An ongoing repository of data on coronavirus cases and deaths in the U.S. [Internet]. GitHub. Available from: https://github.com/nytimes/covid-19-data
12. Impact of opening and closing decisions in the U.S.- Johns Hopkins [Internet]. Johns Hopkins Coronavirus Resource Center. Available from: https://coronavirus.jhu.edu/data/state-timeline
13. Lauer SA, Grantz KH, Bi Q, Jones FK, Zheng Q, Meredith HR, et al. The incubation period of Coronavirus Disease 2019 (COVID-19) from publicly reported confirmed cases: Estimation and application. Annals of Internal Medicine. 2020;172(9):577–82.
14. Burnham KP, Anderson DR. Multimodel inference. Sociological Methods & Research. 2004;33(2):261–304.
15. U.S. Census Bureau, 2020. Available from: https://www.census.gov/en.html
16. Van Vinh Chau N, Lam VT, Dung NT, Yen LM, Minh NNQ, Hung LM, et al. The natural history and transmission potential of asymptomatic severe acute respiratory syndrome coronavirus 2 infection. Clinical infectious diseases: an official publication of the Infectious Diseases Society of America. U.S. National Library of Medicine; 2020. Available from: https://www.ncbi.nlm.nih.gov/pmc/articles/PMC7314145/

17. Arons MM, Hatfield KM, Reddy SC, Kimball A, James A, Jacobs JR, et al. Presymptomatic SARS-COV-2 infections, and transmission in a skilled nursing facility. New England Journal of Medicine. 2020;382(22):2081–90.

18. Richardson S, Hirsch JS, Narasimhan M, Crawford JM, McGinn T, Davidson KW, et al. Presenting characteristics, comorbidities, and outcomes among 5700 patients hospitalized with covid-19 in the New York City area. JAMA. 2020;323(20):2052.

19. Sakurai A, Sasaki T, Kato S, Hayashi M, Tsuzuki S-ichiro, Ishihara T, et al. Natural history of asymptomatic SARS-COV-2 infection. New England Journal of Medicine. 2020;383(9):885–6.

20. Perez-Saez J, Lauer SA, Kaiser L, Regard S, Delaporte E, Guessous I, et al. Serology-informed estimates of SARS-COV-2 infection fatality risk in Geneva, Switzerland. The Lancet Infectious Diseases. 2021;21(4).

21. Wölfel R, Corman VM, Guggemos W, Seilmaier M, Zange S, Müller MA, et al. Virological assessment of hospitalized patients with Covid-2019. Nature. 2020;581(7809):465–9.

22. Andrieu C, Thoms J. A tutorial on adaptive MCMC. Statistics and Computing. 2008;18(4):343–73.

23. Neumann J, Lin YT, Mallela A, Miller EF, Colvin J, Duprat AT, et al. Implementation of a practical Markov chain Monte Carlo sampling algorithm in PyBioNetFit. Bioinformatics. 2022;38(6):1770–2.

Tables

Region	ΔAICc	ΔBIC
Navajo Nation	-6.4	-15.7
Arizona	76.2	66.7
Colorado	108.3	99.1
New Mexico	56.6	47.4
Utah	98.1	89.0

Table 1: Results from our model-selection procedure used to select the number of NPI periods in each region. We calculated the value of the Akaike information criterion corrected for small sample size ($AICc$) for $n = 0$ and $n = 1$ versions of the model, as well as and value of the Bayesian information criterion (BIC) for the same two versions of each model. We defined $\Delta AICc = AICc^{n=0} - AICc^{n=1}$ and $\Delta BIC = BIC^{n=0} - BIC^{n=1}$. We adopted $n = 1$ over $n = 0$ when $\Delta AICc > 10$ and $\Delta BIC > 10$ (i.e., we reject the hypothesis that $n = 0$ when both $\Delta AICc$ and ΔBIC are greater than 10). Accordingly, $n = 0$ is indicated only for the Navajo Nation and $n > 0$ is indicated for all four surrounding states.

445

446 **Figures**

447

448

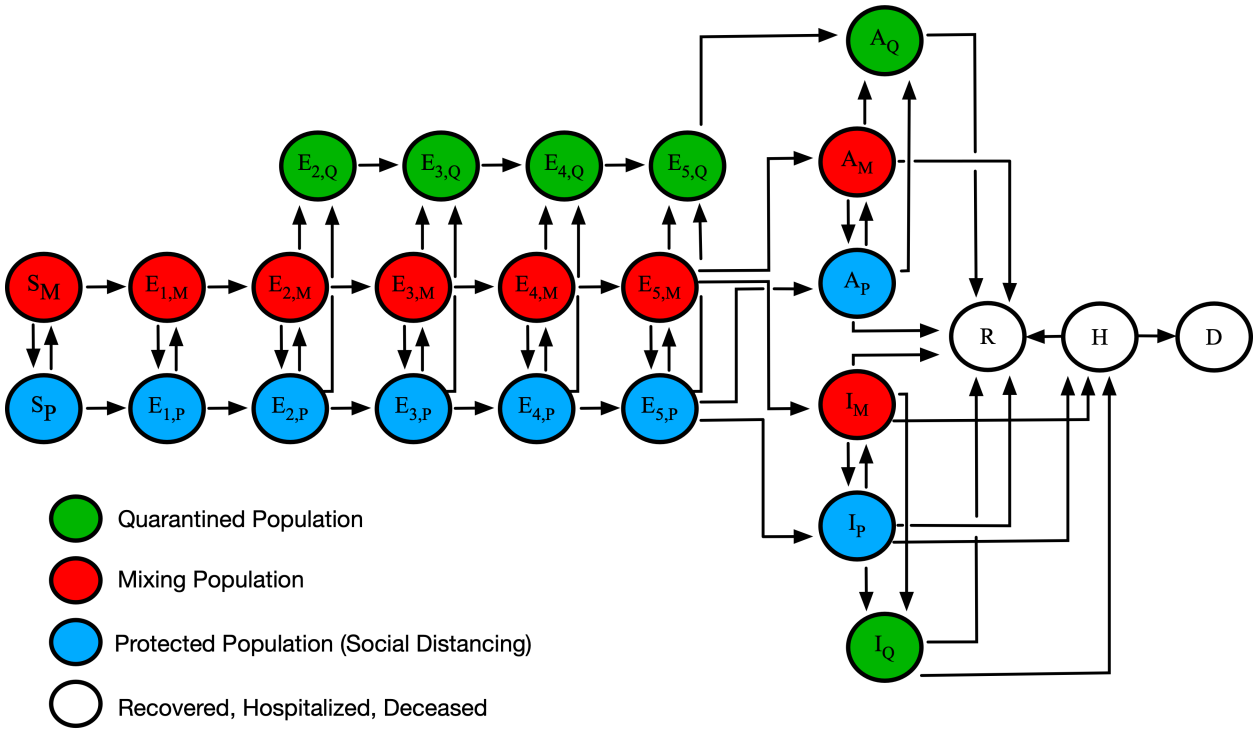

449

450

451 Figure 1: An illustration of the mechanistic compartmental model used to analyze COVID-19
452 data *(7)*. The model captures various subpopulations, as indicated in the legend. Transitions
453 between subpopulations marked by M, P and Q subscripts represent adoption and relaxation of
454 disease-avoiding behaviors. The model accounts for susceptible persons (S), exposed persons not
455 experiencing symptoms while incubating virus (E), asymptomatic persons in the immune
456 clearance phase of infection who never develop symptoms (A), infected persons with mild
457 symptoms (I), infected persons with severe illness (H), deceased persons (D), and recovered
458 persons (R). The incubation period is divided into five stages. Red (subscript M) indicates
459 persons in the mixing population, blue (subscript P) indicates persons in the protected
460 population, green (subscript Q) indicates persons in the quarantined or self-isolated population,
461 and white indicates persons who are recovered, hospitalized, or deceased.

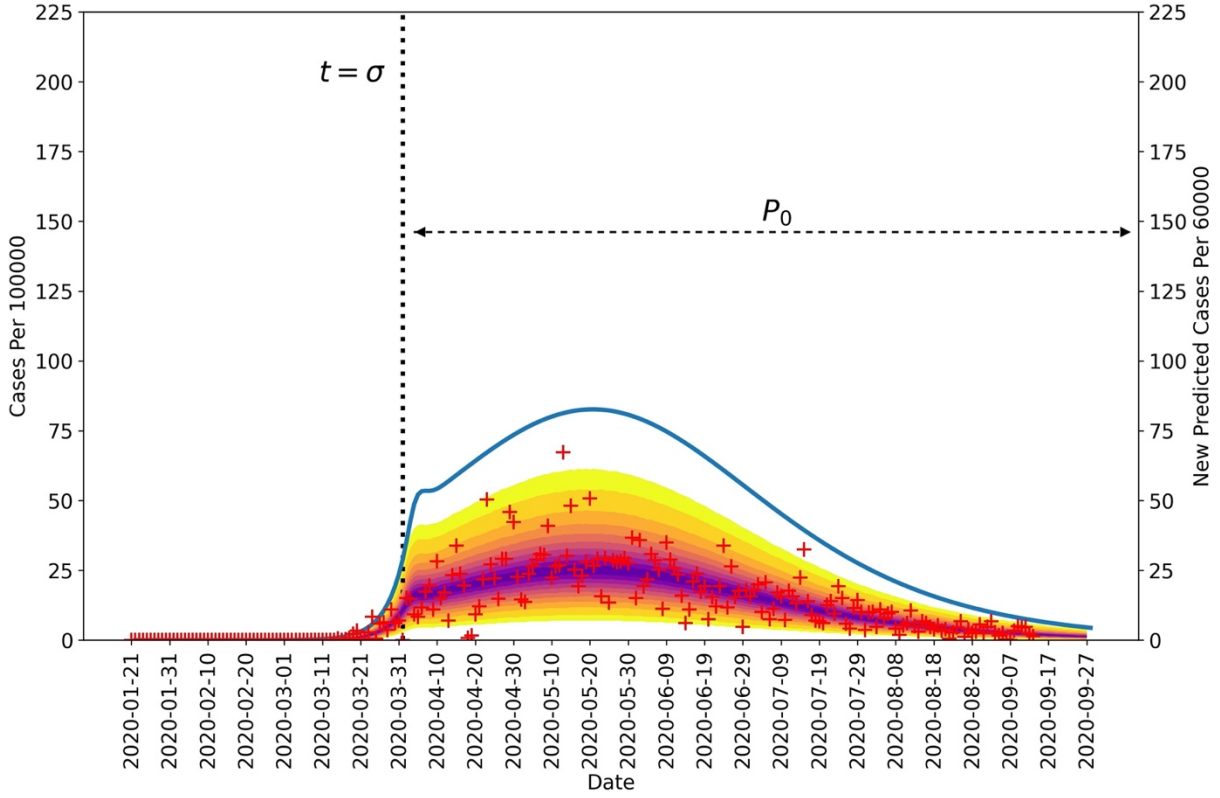

Figure 2: Posterior predictive distribution for new cases detected in the Navajo Nation between 21-January-2020 and 14-September-2020. The daily number of new COVID-19 cases detected in the Navajo Nation are indicated by red markers. The median percentiles of posterior samples are shown in purple. The blue curve indicates daily number of new infections and is based on MAP estimates for model parameters. The vertical black dotted line represents the time at which NPIs began in the Navajo Nation. The horizontal black dotted line indicates the duration of the initial NPI phase. It should be noted that the left and right vertical scales are different.

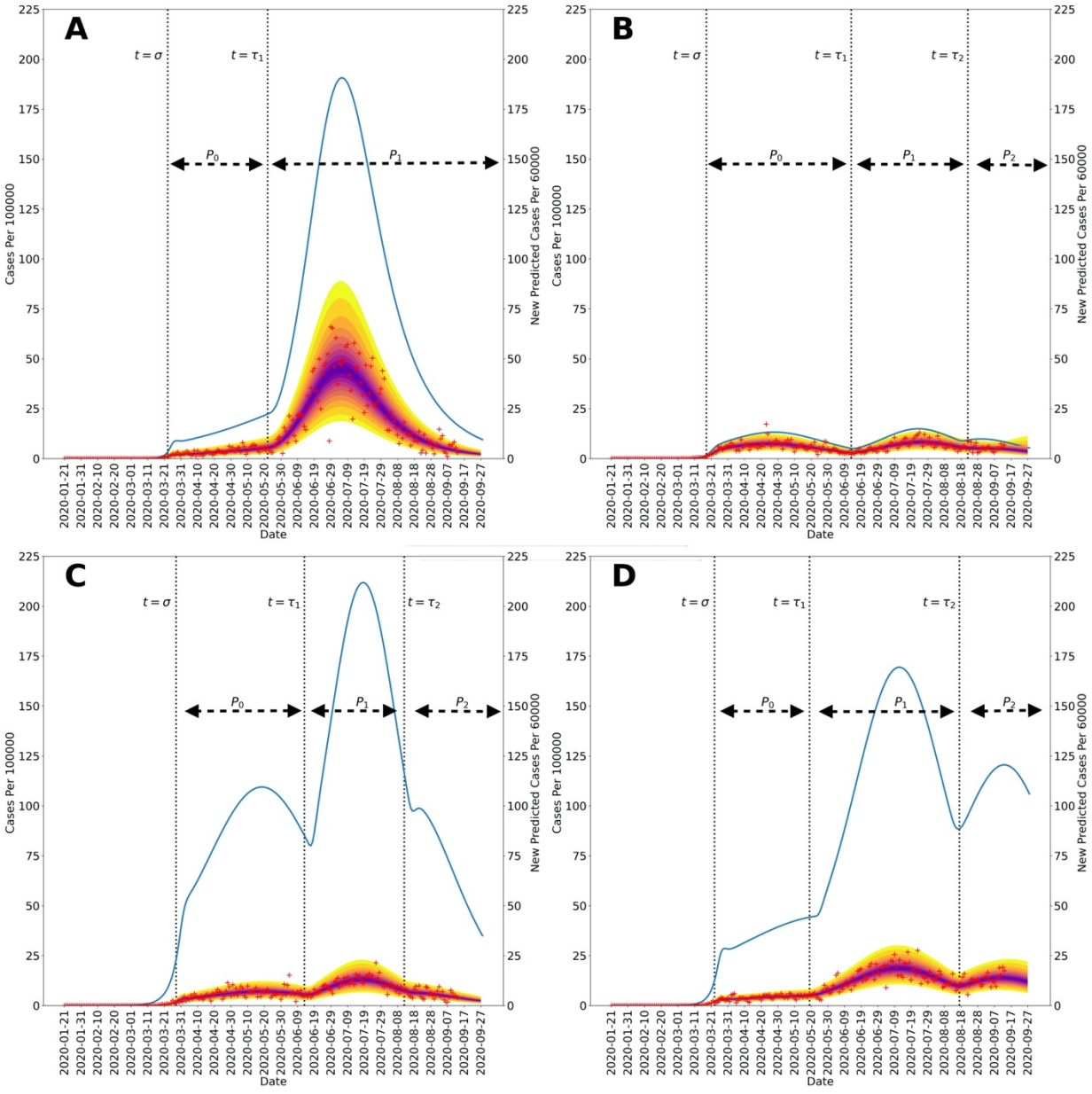

Figure 3: Posterior predictive distributions for new cases in the four US states surrounding the Navajo Nation between 21-January-2020, and 14-September-2020: (A) Arizona, (B) Colorado, (C) New Mexico, and (D) Utah. Recorded region-specific daily new cases of COVID-19 are indicated by red markers in each panel. The median parameter posterior estimates are shown in purple. The yellow bands delimited the 2.5 and 97.5 percentiles; the entire shaded region

indicates the 95% credible interval. In each panel, the blue curve indicates daily number of new infections and is based on MAP estimates for region-specific model parameters. The start times of NPI phases are indicated by vertical dotted lines. The initial NPI phase begins when $t = \sigma$, the second NPI phase begins when $t = \tau_1$, and the third NPI phase begins when $t = \tau_2$. The horizontal black dotted lines indicate durations of NPI phases. It should be noted that the size of the first surge in Arizona, occurring in March and April 2020, is dwarfed by the size of the second surge. It should be noted that the left and right vertical scales of each panel are different.

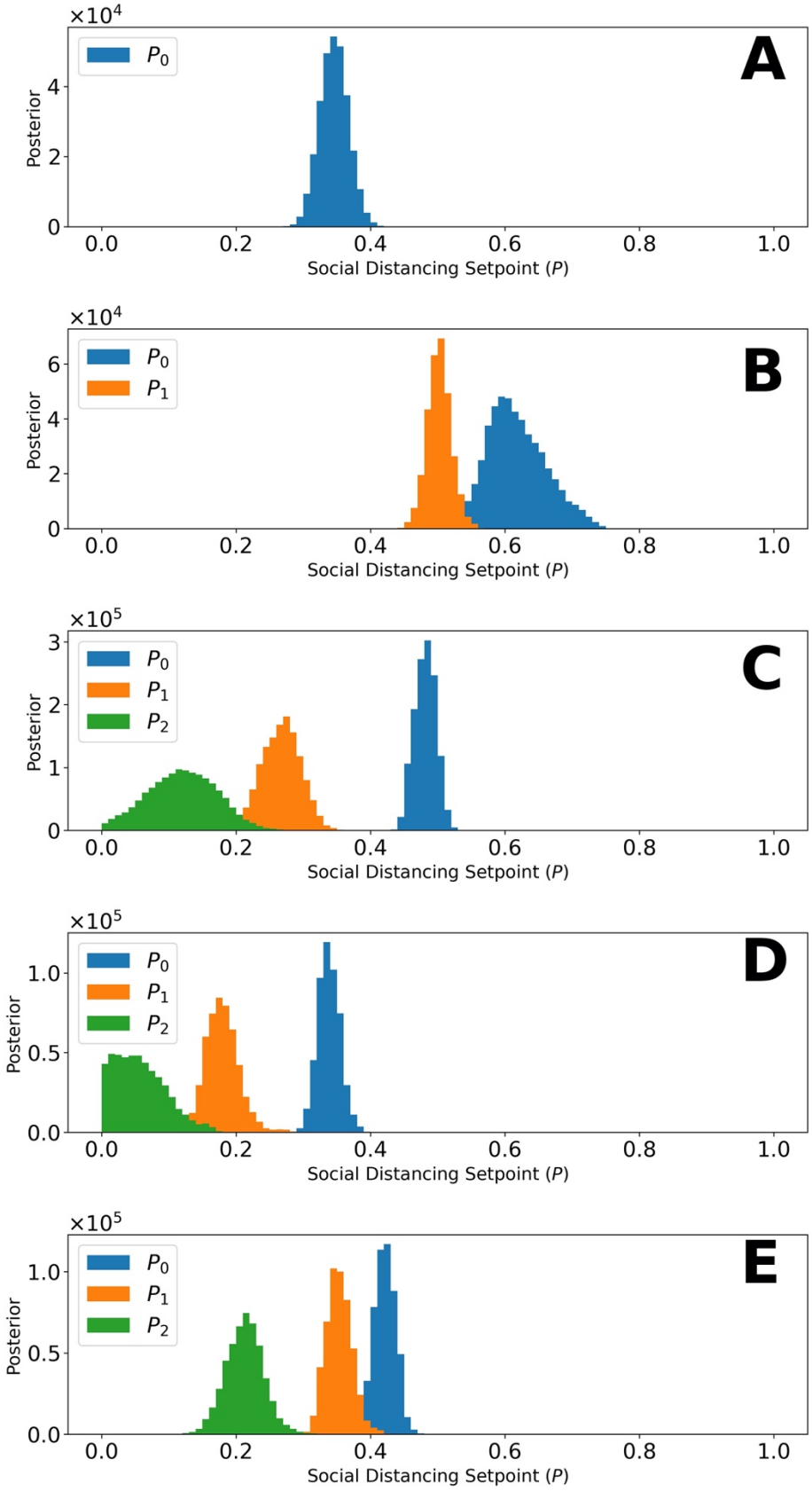

489

Figure 4: Marginal posteriors for parameters of the setpoint function $P_\tau(t)$ (e.g., p_0) for (A) Navajo Nation, (B) Arizona, (C) Colorado, (D) New Mexico, and (E) Utah for the time period January 21, 2020, to September 14, 2020. Recall that $P_\tau(t)$ denotes the fraction of the population practicing disease-avoiding behaviors at time t. The value of $P_\tau(t)$, a step function, is determined by one or more setpoint parameters, denoted p_0, p_1, etc. The Navajo Nation setpoint function parameter has the following maximum a posteriori (MAP) value: $p_0 = 0.35$. The Arizona setpoint function parameters have the following MAP values: $p_0 = 0.60$ and $p_1 = 0.5$. The Colorado setpoint function parameters have the following MAP values: $p_0 = 0.47$, $p_1 = 0.27$, and $p_2 = 0.11$. The New Mexico setpoint function parameters have the following MAP values: $p_0 = 0.34$, $p_1 = 0.19$, and $p_2 = 0.05$. The Utah setpoint function parameters have the following MAP values: $p_0 = 0.43$, $p_1 = 0.35$, and $p_2 = 0.21$ For each region of interest, the NPI switch times, $\tau = \{\tau_1, \ldots, \tau_n\}$, are indicated in Figure 3.

504

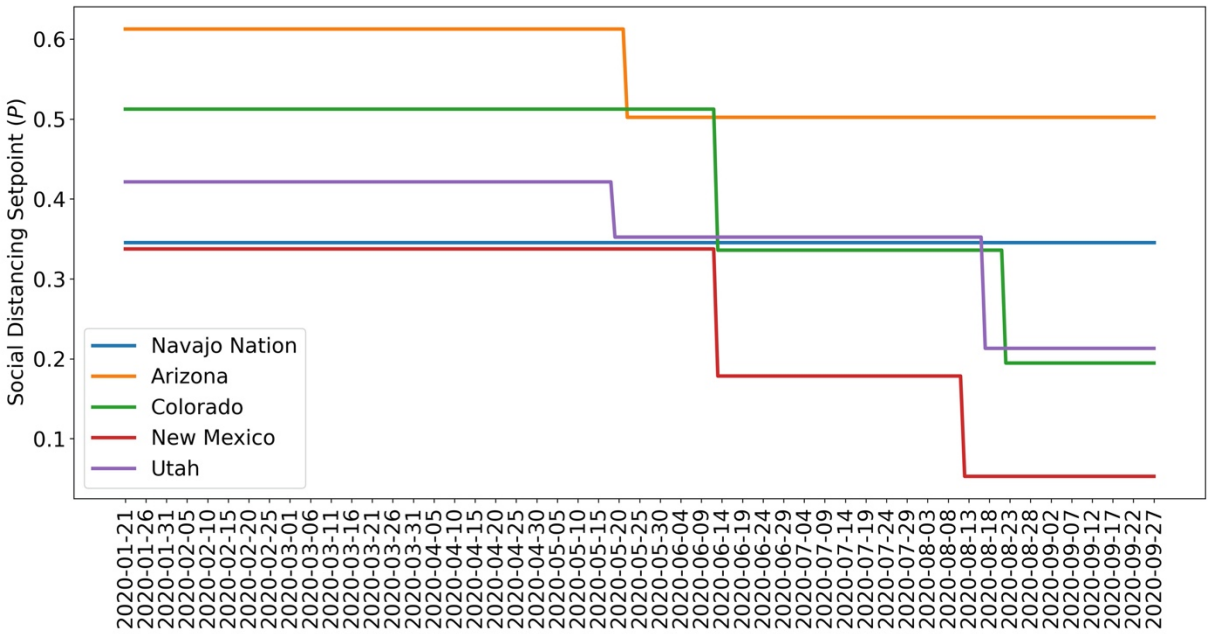

505

506

507 Figure 5: Value of the NPI setpoint function $P_\tau(t)$ over time based on MAP estimates for NPI

508 setpoint parameters $\{p_0, \ldots, p_n\}$ for (A) Navajo Nation (B) Arizona, (C) Colorado, (D) New

509 Mexico, and (E) Utah. The period considered is 21-January-2020 to 14-September-2020.

510

511

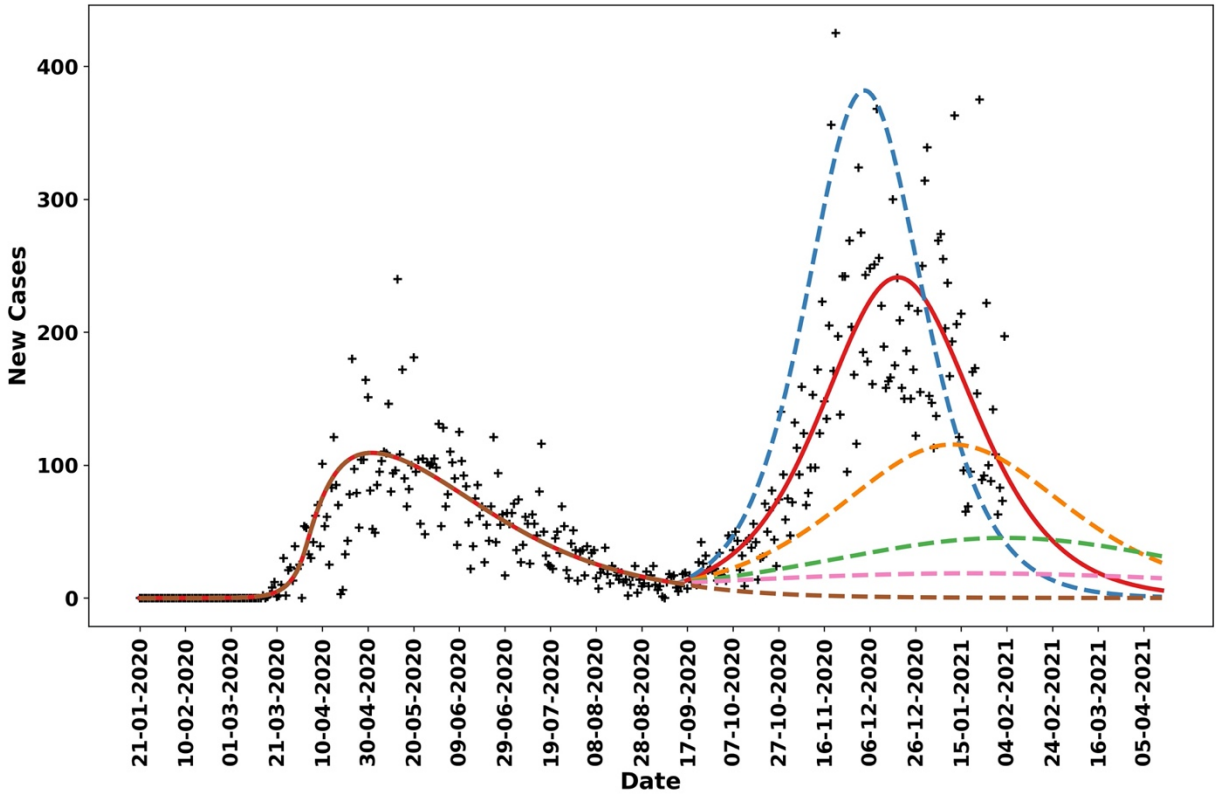

512

513

514 Figure 6: Model-derived projections for various scenarios in which the NPI parameter p_1, which
515 indicates the fraction of the population practicing disease-avoiding behaviors in a second NPI
516 phase in the Navajo Nation starting 14-September-2020, was adjusted to identify the threshold
517 required to prevent a second surge in cases. The red solid line corresponds to the MAP estimate
518 for p_1, which is approximately 0.19. The blue broken line indicates the predicted trajectory for
519 daily cases when p_1 is fixed at 0.15. The orange broken line corresponds to a scenario wherein
520 p_1 is fixed at 0.22, the green broken line corresponds to a scenario wherein p_1 is fixed at 0.25,
521 the pink broken line corresponds to a scenario wherein p_1 is fixed at 0.27, and the brown broken
522 line corresponds to a scenario wherein p_1 is fixed at 0.35.

523

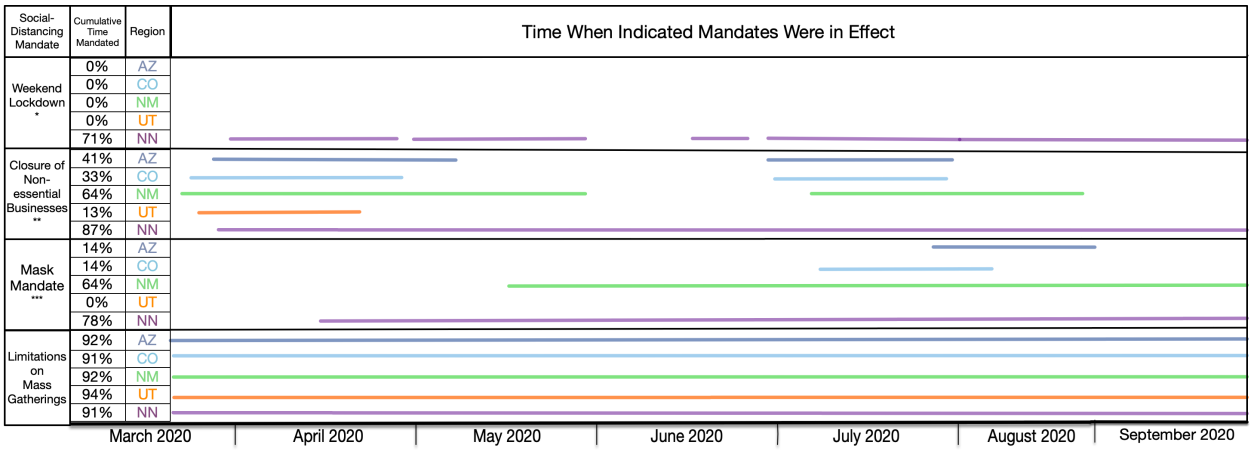

Figure 7: Timeline for mandated NPIs in the Navajo Nation and surrounding states between 01-March-2020 and 14-September-2020. Each region is represented by a different color, as indicated. Only mandates issued by state governors and the president of the Navajo Nation are considered.